Optimisation of FRP Strengthening Systems for Masonry Arch Bridges

Optimisation of FRP Strengthening Systems for Masonry Arch Bridges

M. Daryadel [(1)], L. Cunningham [(2)]
[(1)] *MSc student, School of Mechanical, Aerospace and Civil Engineering, The University of Manchester, Manchester, United Kingdom,* mohammadmahdi.daryadel@postgrad.manchester.ac.uk
[(2)] *Lecturer, School of Mechanical, Aerospace and Civil Engineering, The University of Manchester, Manchester, M13 9PL, United Kingdom,* lee.scott.cunningham@manchester.ac.uk

ABSTRACT
Masonry arch bridges are some of the most common bridge forms in the world. While the majority of these structures are of considerable age, many perform a vital role today carrying roads, rail and services etc. Increased vehicular loads and material deterioration mean that strengthening of existing arches is often required in order to prolong service life. This study will investigate the application of strengthening techniques using fibre reinforced polymer (FRP) composite systems. The application will be explored via numerical modelling using the finite element software package ABAQUS 6.11. The numerical models have been validated with existing experimental test data and are then used to investigate the behaviour of semi-circular masonry arches strengthened with different configurations of FRP e.g. at the intrados, extrados or locally. Then, effects of configuration and amount of FRP on the ductility, strength and global behaviour of strengthened arches will be investigated. Each strengthening system will be compared in terms of increase in strength, ductility, cost and efficiency. Following this, the most efficient strengthening arrangement with the optimum amount of reinforcement will be identified.

KEYWORDS: fibre reinforced polymer composite, finite elements, masonry arches, strengthening.

1. INTRODUCTION

One of the most common types of bridges in the world is the masonry arch. Constructing structures using masonry is a traditional method. Therefore in general, masonry arch bridges tend to have a notable age. These structures were not often designed to carry the equivalent of modern loads e.g. heavy road vehicles, high speed-speed trains etc. In addition to having an essential role as vital pieces of infrastructure, these bridges are often considered as having historic heritage value for many countries. Thus, conservation, retrofitting and strengthening of masonry arch bridges, which can be described as unreinforced masonry (URM) structures, has become a growing area of interest in the past few years. (Grillo, 2003)

In general, lack of theoretical and scientific knowledge in the past has led to constructing these structures based on empirical approaches. In order to extend the service life of existing masonry structures, different traditional techniques for strengthening e.g. application of external/internal steel ties, have been based on existing materials. Although traditional methods enhance the total strength, ductility and stiffness of the structure, URM structures will experience some demerits after traditional strengthening such as increased mass. (Triantafillou, 1998)

Installing fibre reinforced polymer composites offers many benefits to URM structures further to their inherent mechanical characteristics and simplicity of application with minimum disturbance of the structure. With regard to dynamics, the behaviour of the strengthened structure can remain roughly unchanged as application of FRP composites may add a negligible weight and stiffness to the structure, this of course depends on the nature of the FRP system chosen. (Tumailan, et al., 2001)

In the past few years many studies have focused on investigating the behaviour of un-strengthened and strengthened masonry arches. In some cases studies consist of experimental tests accompanied with analytical and/or numerical modelling e.g. (Rovero, et al., 2013), (Borri, et al., 2011), (Cancelliere, et al., 2010), (Oliveira, et al., 2010) , (Borri, et al., 2009), (Bati & Rovero, 2008), (Drosopoulos, et al., 2007), (Ricamato, 2007), (Oliveira, et al., 2006), (Creazza, et al., 2001) and etc. Table 1 gives a summary of some of the mentioned strengthening investigations. To date, most of the previous studies have not explored a wide variation in spatial configuration of the FRP strengthening system. This study intends to provide some insight into the effects of various strengthening configurations.

The aim of the present study is to investigate the behaviour of Glass Fibre Reinforced Polymer (GFRP) strengthened semi-circular masonry arches with a view to developing an optimum FRP strengthening arrangement. The investigation will be conducted via simplified (macro modelling) non-linear finite element (FE) models produced with the commercially available ABAQUS/CAE 6.11 package. Firstly, the FE models are validated in accordance with the results of experimental tests carried out by Basilio (2007). Following this, different approaches of strengthening (e.g. at the intrados, at the extrados or locally) will be compared and the effects of strengthening on the behaviour of the models with different configurations of GFRP strips will be identified.

1.1 Review of modes of failure of un-strengthened masonry arches

As described by Foraboschi (2004), there are a few probable scenarios for failure of a masonry arch:

1. Failure by sliding: In real life, sliding between members is not possible except in the case of a very thick masonry arch. In this case, extreme bending in the line of thrust may cause sliding. Accordingly, as intersections of the thrust line are dependent on hinges in the boundary, the exact place of the thrust line is not identifiable within a thick arch. In this case the sliding load is significantly higher than the load causing formation of hinges.
2. Failure by crushing: The normal action of the cross section is capable of balancing great loads. Failure by crushing is often not probable, i.e., the load causing formation of the hinges is much less than the crushing failure load.
3. Failure due to formation of hinges: This is the most common failure mode whereby the masonry arch fails through formation of four or more hinges in the boundaries (at the intrados or at the extrados).

In view of the aforementioned conditions, there are four possible forms of hinge mechanism for a masonry arch, two of which are not entirely realistic (Figure 1 shape B and shape D). In Figure 1, shape A and shape C are more likely to occur.

1.2 Effects of FRP strengthening on modes of failure

There are five possible failure modes in strengthened masonry arches depending on the geometry of the structure, material properties and applied loads where the first three modes are common with un-strengthened masonry arches (Tao, et al., 2011):

1- Hinge mechanism which is due to rotation of blocks about flexural cracks
2- Crushing due to compressive failure of masonry
3- Sliding of masonry blocks along the shear cracks
4- FRP rupture due to severe tensile forces
5- Debonding of FRP due to separation in adhesive joints

Using FRP systems modifies the failure behaviour of masonry arches significantly and enhances the load-bearing capacity of the structure. FRP systems make masonry capable of carrying tensile stresses and thus improve the biggest deficiency of masonry structures. Usually, formation of the fourth hinge leads to a brittle collapse. This brittle collapse mechanism, the most common failure mode for un-strengthened masonry arches, can be possibly prevented through the application of FRP systems. Accordingly, the thrust line, the line of action of resultant compressive forces, is limited to the outer edge of the arch by using extrados FRP strengthening [Figure 2 (a)]. In the former mentioned case formation of the fourth hinge is prevented. Conversely, through intrados strengthening, the thrust line moves out of the voussoir and the number of hinges is limited to three [Figure 2 (b)]. Consequentially, collapse is due to other mechanisms e.g. FRP rupture, FRP debonding or masonry crushing. (Borri, et al., 2009)

However, both approaches of strengthening (at the intrados or at the extrados) with FRP prevent the hinge mechanism; in most cases the extrados of the arch may not be accessible. In some rare cases where aesthetic aspects of the structure constrain the strengthening procedure, strengthening at the intrados may not be feasible (Tao, et al., 2011).

Of the failure mechanisms mentioned above, debonding of FRP is not probable when FRP strips are applied at the extrados of the arch as normal stresses on the FRP-masonry interface are beneficial. In this case, experimental tests show that the most likely failure mechanism is due to sliding of the masonry. On the other hand, in the case of applying FRP at the intrados, debonding of the FRP is more likely to happen near the supports or under the concentrated load. Following the debonding of the FRP, experiments show the structure fails due to the hinge mechanism identical to the un-strengthened arch. Moreover, in a masonry arch strengthened at the intrados, the collapse mechanism is due to crushing (compressive failure of masonry) assuming that no debonding occurs. Debonding may occur in different forms. In most cases, epoxy resin has much higher tensile strength in comparison with masonry. Hence generally, debonding of the FRP happens with local tensile failure of masonry. As experiments demonstrate, a layer of the masonry can be ripped or a block of masonry can possibly be pulled out and remains attached to the FRP. Debonding of the FRP plays a vital role in the global behaviour of the strengthened masonry arches as it can significantly influence the failure mechanism of the structure. (Drosopoulos, et al., 2007)

2. NUMERICAL MODELLING OF UN-STRENGTEHEND AND STRENGTHENED MASONRY ARCHES

In order to investigate optimum arrangements of FRP strengthening, numerical modelling using non-linear finite element analysis is conducted. For the purpose of validating the finite element models, semi-circular scaled masonry arches used in experiments published by Basilio (2007) were modelled using ABAQUS 6.11. These 1.5m span arches were tested with a knife edge loading (with the rate of 5μm/s) applied at quarter span. The geometry of the arches is identical and shown in Figure 3. The macro modelling method was used to simulate the masonry structure, i.e. the masonry and mortar were treated as one continuum, and the composite materials were modelled using the macromechanics method. According to the aim of this study, the FRP-masonry interface is assumed to be perfectly fixed and no debonding occurs. Consequently, a tie constraint is assigned to the FRP-masonry interface in ABAQUS where the masonry is the master surface and FRP is the slave surface. The discretization method for the defined constraint is “surface to surface”. Material properties of the masonry and GFRP strips were obtained from experimental tests carried out by Basilio (2007) and are given in Table 2.

According to Harvey (2010), for the numerical simulation of brittle materials, the concept of damage mechanics appears to be fairly accurate. Generally, masonry can be treated as a two phase material which constitutes a brittle elastic component (brick or stone) and a component (mortar) which shows an inelastic strain caused by plasticity or damage phenomena. Thus, material properties of masonry as a macroscopically orthotropic material can be defined using the concrete damage plasticity module in ABAQUS where according to Basilio (2007) the dilation angle is equal to 36.87º and eccentricity is equal to 0.023. Where some parameters (e.g. Viscosity parameter) were not defined by Basilio (2007), default ABAQUS values were used.

For calculating the inelastic compressive strain of masonry Kaushik, et al.(2007) suggests a relationship where the ultimate strain is assumed to be 0.00525. Genikomsou and Polak (2015) suggest a tensile stress-strain relationship for concrete andsince the characteristics of masonry and concrete are similar, the aforementioned relationship is used for calculating the ultimate tensile strain in the masonry (0.000433).

The masonry arches are modelled as a whole using 3D finite elements, which are 20-node quadratic brick elements (type C3D20R) with an element size of 25 mm within the mesh. It should be noted that mesh sensitivity analyses were carried out before choosing the mentioned mesh size and type. Figure 4 shows the force-displacement graph from experimental results and numerical modelling of an arch strengthened at the extrados (specimen CSE2) tested by Basilio (2007). The present model was able to achieve a reasonable level of accuracy, in particular the prediction of post-peak behaviour and the failure mode. Further validation studies of the present model are given in Daryadel (2015).

3. INVESTIGATION OF DIFFERENT STRENGTHENING CONFIGURATIONS

In order to identify the best arrangement for each system (strengthened at the intrados, extrados or locally) peak force, maximum displacement corresponded to peak force and kinematic ductility of each model is examined. To evaluate the efficient amount of reinforcement, different widths of FRP are used for each system. Also, the utilization factor (U.F.) is introduced, this being the value of maximum stress in FRP at peak force divided by the total amount of FRP used in the model and its unit is N/mm^4.

3.1 Local strengthening system

To explore the behaviour of locally strengthened masonry arches with GFRP strips, 12 FE models are created. In this paper, local strengthening refers to the case where the FRP strips are not continuous along the full length of the extrados or intrados. Details of the reinforcement in individual models are listed in Table 3. Herein, models are strengthened with GFRP strip(s) at the intrados under the loading point and at the extrados symmetric to the loading point (Figure 5). The

aim of this strengthening approach is to prevent the formation of the first two hinges and enhance the strength and ductility of models with minimum amount of reinforcement. Figure 6 depicts the force-displacement graph of LL and LT models. Value of kinematic ductility for each model is calculated and presented in Figures 7 and 8.

The following can be concluded from the LT and LL models:

1. Using localized strengthening in the longitudinal direction is more effective than the transverse direction.
2. Considering the same amount of reinforcement, applying two strips of reinforcement leads to higher peak forces
3. Locally applying reinforcement to un-strengthened masonry arches does not always improve the global behavior and might worsen brittle behaviour.
4. Increasing the amount of reinforcement is not always favourable

3.2 Strengthening at the intrados

To investigate the behaviour of strengthened masonry arches at the intrados, 6 models are created. Details of the reinforcement used in the models are given in Table 4. It should be pointed out that GFRP strip is applied to the middle of the cross section at the intrados of IN1-1, IN1-2 and IN1-3. Also, Centre to centre distances of GFRP strips in IN2-1, IN2-2 and IN2-3 are 150 mm and reinforcement is applied symmetrically on the surface of the intrados which is 450 mm wide.

The goal of strengthening URM arches at the intrados is to modify the static behaviour of the structure and alter the brittle failure mechanism by preventing the fourth hinge from being formed. In addition, this system is the most feasible solution of strengthening masonry arches with the shortest required time and the lowest effort and cost since the intrados is more accessible than the extrados of arch bridges due to the presence of backfill. (Hollaway & Teng, 2008)

Figure 9 illustrates the applied force-displacement graph for 6 strengthened models at the intrados and the un-strengthened model. Value of kinematic ductility for each model is calculated and presented in Figure 10.

The following can be deducted from IN models:

1. Expanding the width of FRP strips enlarges the peak force
2. Applying excessive amount of FRP may decrease the peak displacement
3. Considering the same amount of reinforcement, applying two strips of reinforcement leads to higher peak forces, peak displacements and kinematic ductility
4. Spreading out the same amount of FRP along a section increases the maximum elastic displacement.

3.3 Strengthening at the extrados

To investigate the behaviour of strengthened masonry arches at the extrados, 6 models are created. Details of the reinforcement used in the models are given in Table 5. It should be pointed out that the GFRP strips are applied to the middle of the cross section at the extrados of EX1-1, EX 1-2 and EX 1-3. Centre to centre distances of GFRP strips in EX 2-1, EX 2-2 and EX 2-3 are 150 mm and reinforcement is applied symmetrically on the surface of the extrados.

The goal of strengthening URM arches at the extrados is to modify the brittle behaviour, enhancing the load bearing capacity and increasing the maximum displacement of the structure by pushing the line of thrust out of the extrados.

According to the results of experimental tests by Basilio (2007), strengthening masonry arches at the extrados increases peak force and peak displacement more than strengthening at the intrados. As previously mentioned, the extrados is not always accessible in bridges however strengthening at the extrados is a feasible solution mostly in the case of the vaults and domes in buildings (Hojdys & Krajewski, 2012).

Figure 11 shows the applied force-displacement graph for 6 strengthened models at the extrados along with the un-strengthened model. Value of kinematic ductility for each model is calculated and presented in Figure 12.

The following can be concluded from EX models:

1. Spreading out the same amount of reinforcement at the extrados decreases kinematic ductility
2. Considering the same amount of FRP, using two strips increases the peak displacement more than one strip
3. The value of maximum elastic displacement does not follow any specific trend in different EX models.

3.4 Strengthening at the intrados, various configurations

Comparing all the strengthening systems, strengthening at the intrados with FRP strips is a more viable approach. Herewith, further investigation of strengthening arrangements for the intrados is required. Hence, 6 different models are created with different arrangements of GFRP strips at the intrados. Reinforcement details of these models are presented in Table 6.

First three models (D1, D2 and D3) are strengthened with 2 diagonal strips along the intrados. For instance, Figure 13 shows the attached diagonal GFRP strips of model D1. Model SH is strengthened with a GFRP sheet applied to the whole intrados. Models GR1 and GR2 are strengthened with a grid of GFRP strips at the intrados. Figure 14 shows the attached GFRP grids.

Figure 15 shows the applied force-displacement graph for D, SH and GR models. Value of kinematic ductility for each model is calculated and presented in Figure 16.

The following can be summarized as the conclusions of D, GR and SH models in this section:

1. In the D models, by expanding the width of reinforcement, the peak load increases and both corresponding peak displacement and kinematic ductility decrease.
2. In the GR models, by widening the reinforcement, and decreasing the total amount of GFRP, the peak load decreases and both corresponding peak displacement and kinematic ductility increase.
3. Using GFRP sheet at the intrados does not modify the brittle behaviour of the masonry arches and only increases the strength of the structure.

4. COMPARISON BETWEEN STRENGTHENING SYSTEMS

As described by Hollaway and Teng (2008), applying FRP at the intrados of the masonry arches is the most feasible solution. Therefore, strengthening systems which involve applying reinforcement at the extrados are not considered for further investigations although they are able to increase the strength and ductility of masonry arches significantly e.g. EX2-3 by 461.33%, 1797.06% and 300% increase in peak load, peak displacement and kinematic ductility respectively. In the IN models, IN2-2 (2 strips of 50 mm wide) has the highest peak displacement. Comparing IN1-2 and IN2-2 shows that with the same amount of reinforcement, IN2-2 has higher increase in peak load, peak displacement and kinematic ductility in addition to having a larger U.F. Moreover, making a comparison between IN2-2 and IN2-3 proves the fact that IN2-2 is the most efficient model. In this regard, it should be pointed out that the increase in peak force of IN2-3 is only 114% higher than that of IN2-2 while

using twice the amount of FRP used in IN2-2. On the other hand, increase in peak displacement of IN2-2 is 111.77% higher than that of IN2-3.

In the D models, D2 has the highest peak displacement and kinematic ductility. Although the amount of FRP used in D3 is twice the amount of FRP used in D2, increase in peak load of D3 is just 117.12% higher than that of D2. Furthermore, peak displacement, kinematic ductility and U.F. of D2 are higher than those of D3. Hence, it can be concluded that D2 is the most efficient model in the D series. A brief review of the results of GR and SH models verifies the fact that GR2 is the most efficient model considering the amount of FRP used and the resulting increase in peak force, peak displacement and kinematic ductility.

In order to identify the most efficient strengthened model at the intrados, numerical results of IN2-2, D2 and GR2 are to be compared. Also, a new parameter is introduced and described which will consider the price per metre length of each strengthening system.

For a better view on the relative cost of strengthening an approximate calculation is carried out for three chosen models. The procedure follows that of Burgoyne (2004) where two cost ratios are defined based on the ultimate strength and stiffness of materials. To calculate the mentioned cost ratios, the cost of different materials is first estimated based on 1£/kN/metre (cost ratio of providing strength) and 1£kN/mm of extension/m length of the material (cost ratio of providing stiffness). Note that calculated costs did not consider the labour and anchorage costs and were based on charges in the UK in 2004. Also, it should be noted that aim of Burgoyne (2004) was to estimate the cost of using FRP in design in comparison with common materials such as steel and anticipate the future of FRP in the market. This work was further extended by Burgoyne and Balafas (2007). It was concluded that the design of structures using advanced composite materials is highly dependent on the world economics. Consequently, financial consideration in design of structures using advanced composites plays a crucial role since the price of FRP composites remain relatively high. Thus, to have a broader view for an effective and efficient design of strengthening systems, financial issues are considered in this study.

The aim of strengthening masonry arch bridges using FRP composites is more related to providing higher ultimate strength. Consequently, the price of providing stiffness for the chosen models is not calculated and only the price of providing strength is used in the following calculations.

For GFRP, the cost of providing strength is 0.013 (£/kN/m) where for instance, this value for pre-stressing steel is 0.002 (Burgoyne, 2004). Multiplying 0.013 (£/kN/m) by the maximum stress (MPa) in GFRP (at the point the model is experiencing its peak load) gives the price per volume of GFRP. Then, by multiplying the resultant value by the total amount of GFRP (mm^2) used in the model a rough estimation of the strengthening cost per unit length of model can be calculated. It should be noted that this value is only a mean for the purpose of comparison and might be different in the current market. For example, the strengthening price of model IN2-2 is calculated as follows:

$$P_{IN2\text{-}2}=0.013(£/kN.m)\times 57.18(N/mm^2)\times 201585(mm^2)=149.85(£/m)$$

Similarly, the price per unit length of the models D2 and GR2 are calculated. For an easier comparison, an overall point for each model is calculated as:

Overall point = (increase in peak load) + (Increase in peak displacement) + (increase in kinematic ductility) + (U.F×100) - (price per unit length)

Numerical results, price per unit length and overall points of IN2-2, D2 and GR2 are presented in Table 7.

GR2 has the highest increase in kinematic ductility and peak displacement however the U.F. of this model has the smallest value. Price per unit length of this model is much higher than that of D2 and IN2-2. Collectively, this approach of strengthening does not seem to be the most efficient model as its overall point is the smallest (1395.93 points).D2 has the highest U.F. (5.8 $N/mm^4 \times 10^{-4}$) while that of IN2-2 is 2.84 ($N/mm^4 \times 10^{-4}$). Also, the increase in kinematic ductility and peak displacement for D2 is larger than those of IN2-2 albeit the increase in peak load for IN2-2 is higher than that of D2 (214.55% and 182.54% respectively).

The results of this study indicate that, D2 seems to be the most efficient model considering increased strength and ductility together with relative cost aspects.

5. CONCLUSION

Before starting the design process of the strengthening system for URM arches, it is necessary to have a clear understanding of the likely behaviour of the strengthened structure. Minor changes in the strengthening approach and/or the amount of reinforcement used in each strengthening system can lead to notable differences in the behaviour. Thus, this study focussed on identifying the differences between various strengthening approaches using different widths of FRP strips and spatial arrangements.

Selection of the strengthening method in the design procedure is limited by a number of constraints. Depending on the desired, available and residual strength and repair scheme, the goal of strengthening varies. Concerning this, other factors such as ductility, budget limitations, physical and time constraints all play a part. (Islam, 2008)

After assessment of the URM arch and considering all the mentioned factors, one of the described strengthening approaches can be used. This study explored and presented the increase in strength and ductility of each strengthening system to provide a view for an efficient retrofitting design using FRP.

For the localised strengthening system (LL and LT models), effects of the direction, width and number of strips of FRP were investigated. Henceforth, the outcomes of this investigation are summarized as below:

- Using the reinforcement in the longitudinal direction is more effective than the transverse direction.
- Spreading out the same amount of FRP along the section increases the peak force.
- Using excessive amount of FRP could exacerbate brittle behaviour.
- Local strengthening might lead to unfavourable changes.

Investigation of strengthening the extrados (EX models) was carried out using the same approach as the intrados with each location producing different results . The following can be concluded:

- Widening the FRP strip(s) increases the peak force.
- Widening the FRP strip(s) decreases the peak displacement.
- Applying one strip of the FRP is more effective than 2 strips at increasing the kinematic ductility.
- Spreading out the same amount of FRP along the width of the arch increases the peak displacement more than using one strip of reinforcement.

Investigation of strengthening the intrados was carried using different numbers and widths of FRP strips (IN models). Also, diagonal FRP strips with three different widths were applied to the intrados (D models). Applying the strips diagonally was found to be the most efficient approach. Results of this exploration are summarized as follows:

- Widening the FRP strip(s) increases the peak force.

- Spreading out the same amount of FRP along the section increases the maximum elastic displacement.
- Applying the same amount of FRP, using two strips is more efficient than one strip.
- Applying excessive amount of FRP decreases ductility and peak displacement.
- Assuming the same amount of FRP in IN and D models, D models illustrate more ductile behaviour

For additional investigations on strengthening the intrados, FRP sheet and grids were also used. Depending on the practical constraints/goals of the strengthening, these systems could be proposed. Outcomes are listed below:

- Reducing the void surfaces in the FRP grid leads to larger peak displacement and kinematic ductility.
- Peak force increases by increasing the amount of FRP

Overall, the most efficient intrados strengthening system was found to be the diagonally placed strips denoted by model D2. This is based on the consideration of the % increase in peak load, ductility, FRP utilisation and relative cost. The work presented here focussed on arches of one geometry and load arrangement, further investigation varying these properties is needed. In view of the limitations of the macro modelling approach used in this work, physical testing of the preferred strengthening arrangements is recommended as a means of further exploration. Similarly, more sophisticated numerical models adopting a micro modelling approach in addition to surface contact may be used to investigate de-bonding phenomena for the chosen strengthening arrangements.

REFERENCES

Basilio, I., 2007. *Strengthening of arched masonry*, Guimaraes: University of Minho, Department of Civil Engineering.

Bati, S. B. & Rovero, L., 2008. Towards a methodology for estimating strength and collapse mechanism in masonry arches strengthened with fibre reinforced applied on external surface. *Materials and Structures*, Volume 41, pp. 1291-1306.

Borri, A., Casadei, P., Castori, G. & Hammond, J., 2009. Strengthening of Brick Masonry Arches with Externally Bonded Steel Reinforced Composites. *Journal of Composites for Construction*, Volume 13, pp. 468-474.

Borri, A., Castori, G. & Corradi, M., 2011. Intrados strengthening of brick masonry arches with composite materials. *Composites*, 428(5), pp. 1164-1172.

Burgoyne, C.J., 2004. Does FRP have an economic future?. In: *Advanced Composite Materials in Bridges and Structures – ACMBS IV,* Calgary, Alberta, July 20-23

Cancelliere, I., Imbimbo, M. & Sacco, E., 2010. Experimental tests and numerical modeling of reinforced masonry arches. *Engineering Structures*, Volume 32, pp. 776-792.

Creazza, G., Saetta, A. V., Matteazzi, R. & Vitaliani, R. V., 2001. *Analysis of masonry structures reinforced by FRP.*

Daryadel, M., 2015. *Strengthening of masonry arch bridges with fibre reinforced polymer composites*, MSc. Dissertation, University of Manchester, School of Mechanical Aerospace and Civil Engineering.

Drosopoulos, G., Stavroulakis, G. & Massalas, C., 2007. FRP reinforcement of stone arch bridges: Unilateral contact models and limit analysis. *Composites*, Volume 38, pp. 144-151.

Foraboschi, P., 2004. Strengthening of Masonry Arches with Fiber-Reinforced Polymer Strips. *Journal of Composites for Construction*, Volume 8, pp. 191-200.

Genikomsou, A. S. & Polak, M. A., 2015. Finite element analysis of punching shear of concrete slabs using damaged plasticity model in ABAQUS. *Engineering Structures*, Volume 98, pp. 38-45.

Grillo, V. E., 2003. *FRP/Steel Strengthening of unreinforced concrete masonry piers*, Florida: University of Florida.

Harvey, W., 2010. Briefing: Spreadsheet analysis of complex masonry structures. *Engineering and Computational Mechanics*, 163(EM3), pp. 125-128.

Hojdys, L. & Krajewski, P., 2012. Experimental tests on strengthened and unstrengthened masonry vault with backfill. *Journal of Heritage Conservation*, pp. 105-108.

Hollaway, L. & Teng, J.-G., 2008. *Strengthennig and rehabilitation of civil infrastructures using fibre-reinforced polymer (FRP) comosites*. Cambridge: Woodhead publishing.

Islam, M. R., 2008. *Inventory of FRP strengthening methods in masonry structures*, Barcelona: Technical University of Catalonia.

Kaushik, H. B., Rai, D. C. & Jain, S. K., 2007. Stress-Strain Characteristics of Clay Brick Masonry under Uniaxlia Compression. *Journal of Materials in Civil Engineering*, September, 19(19), pp. 728-139.

Oliveira, D., Basílio, I. & Lourenço, P., 2006. *FRP strengthening of masonry arches towards an enhanced behavior.* s.l., Taylor & Francis.

Oliveira, D. V., Basilio, I. & Lourenço, P. B., 2010. Experimental Behavior of FRP Strengthened. *Journal of Composites for Construction*, Volume 13, pp. 312-320.

Ricamato, M., 2007. *Numerical and experimental analysis of masonry arches strengthened with FRP*, Cassino: University of Cassino.

Rovero, L., Focacci, F. & Stipo, a. G., 2013. Structural Behavior of Arch Models Strengthened Using Fiber-Reinforced Polymer Strips of Different Lengths. *Journal of Composites for Construction*, Volume 17, pp. 249-257.

Tao, Y., Stratfor, T. & Chen, J., 2011. Behaviour of a masonry arch bridge repaired using fibre-reinforced polymer composites. *Engineering Structures*, Volume 33, pp. 1594-1606.

Triantafillou, T. C., 1998. Strengthening of Masonry Structures Using Epoxy-Bonded FRP. *Journal of Composites for Construction*, Volume 2, pp. 69-103.

Tumailan, G., Antonio, N., Modena, C. & Morbin, A., 2001. *Shear Strengthening of Masonry Walls with FRP Composites*. Tampa, Composites Fabricators Association.

FIGURES

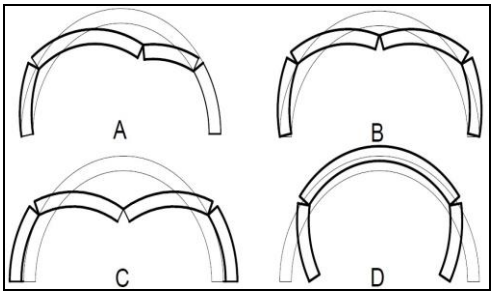

Figure 1: Typical failure modes in masonry arches, based on Foraboschi (2004)

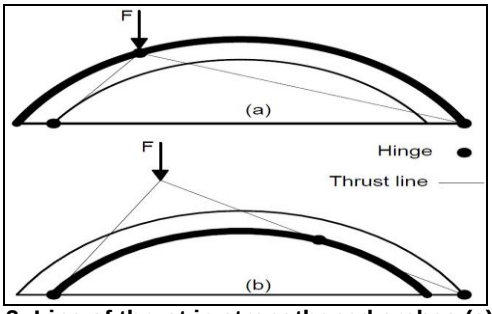

Figure 2: Line of thrust in strengthened arches (a) at the extrados (b) at the intrados, based on Borri et al. (2009)

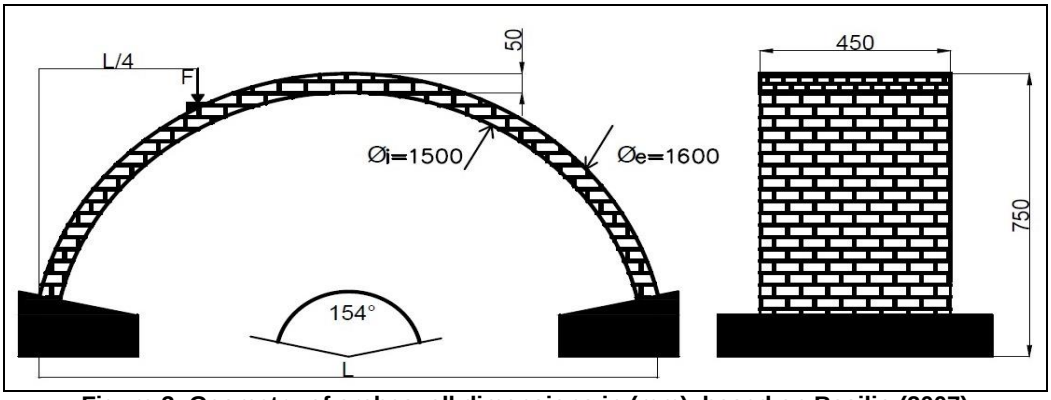

Figure 3: Geometry of arches, all dimensions in (mm), based on Basilio (2007)

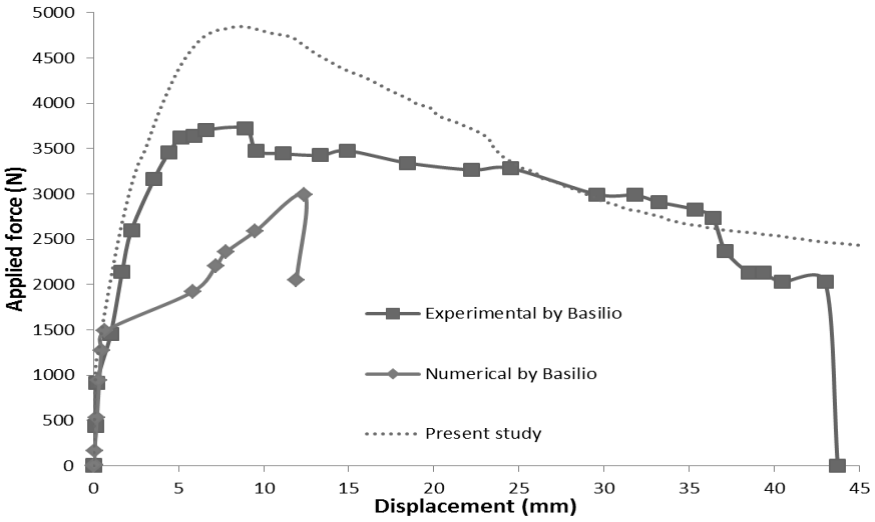

Figure 4: Force versus displacement at the loading point for arch CSE2

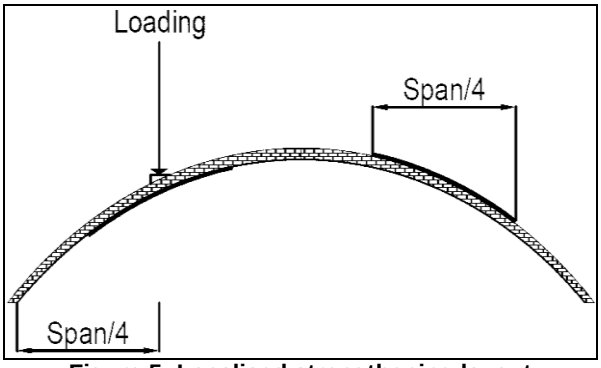

Figure 5: Localised strengthening layout

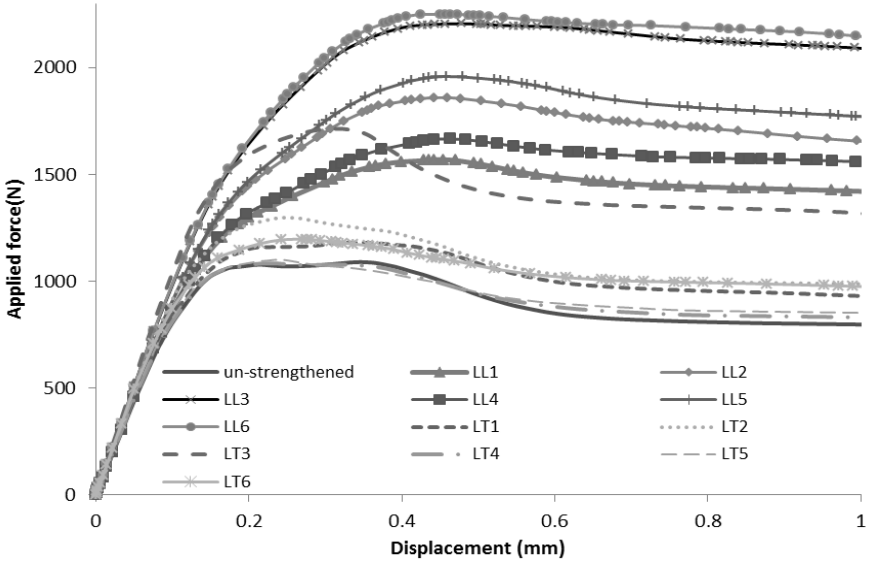

Figure 6: Applied force versus displacement for locally strengthened ABAQUS models

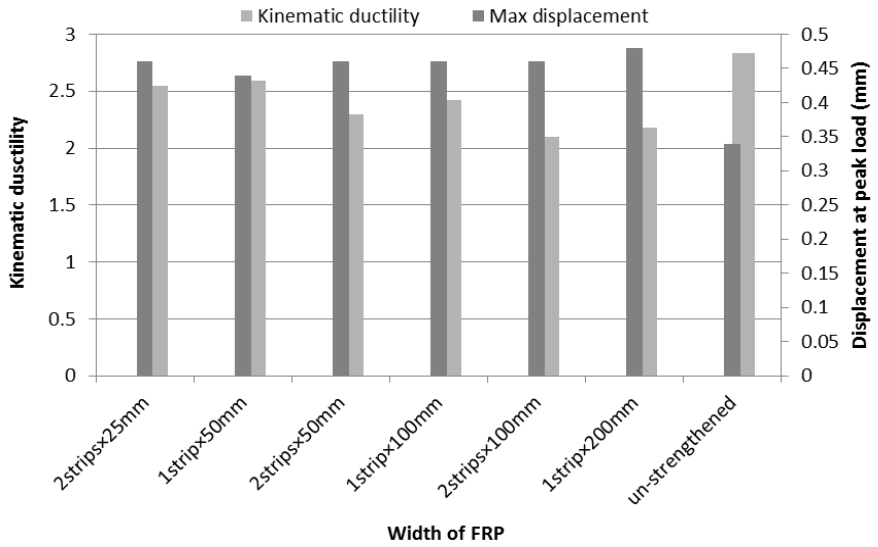

Figure 7: Kinematic ductility/peak displacement versus width of FRP for LL models

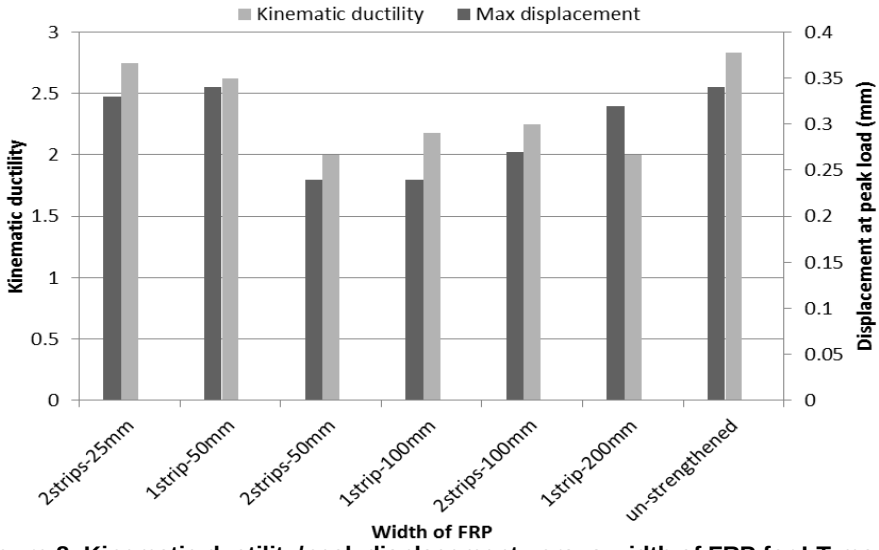

Figure 8: Kinematic ductility/peak displacement versus width of FRP for LT models

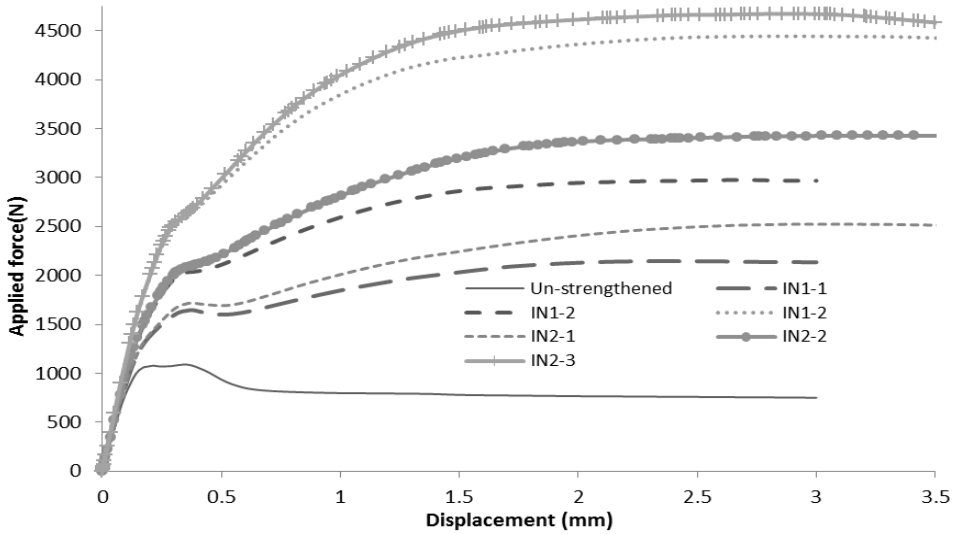

Figure 9: Applied force versus displacement for IN models

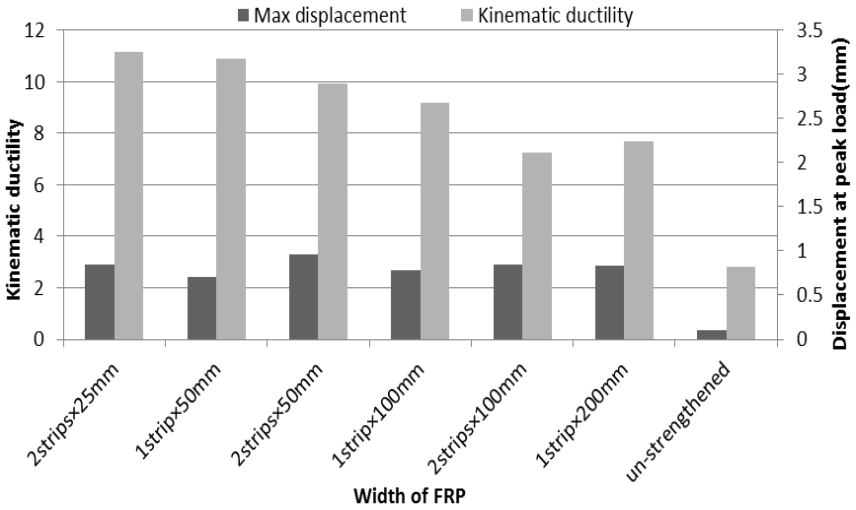

Figure 10: Kinematic ductility/peak displacement versus width of FRP for IN models

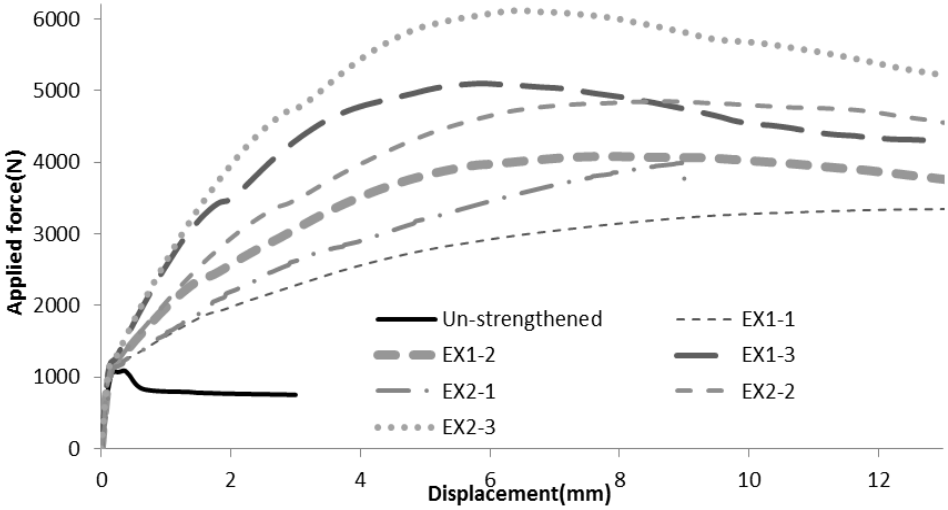

Figure 11: Applied force versus displacement for EX models

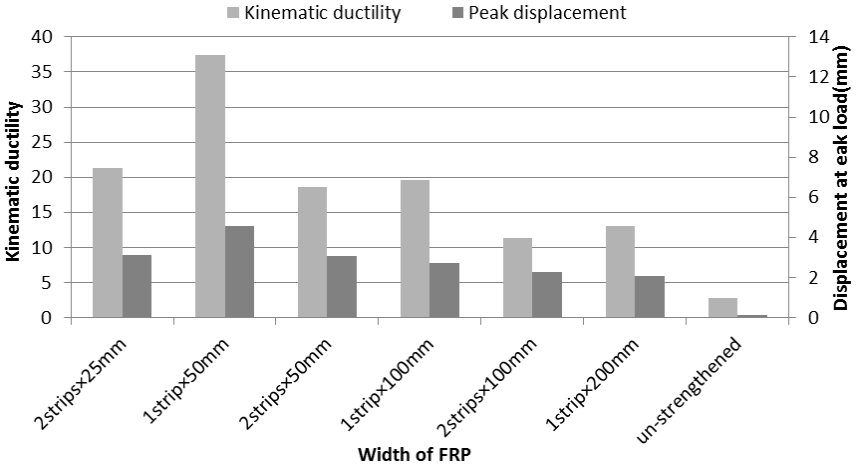

Figure 12: Kinematic ductility/peak displacement versus width of FRP for EX models

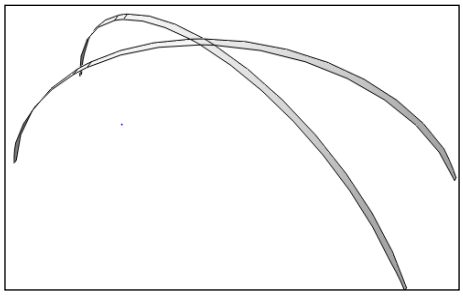

Figure 13: Diagonal GFRP strips applied to the intrados, model D1

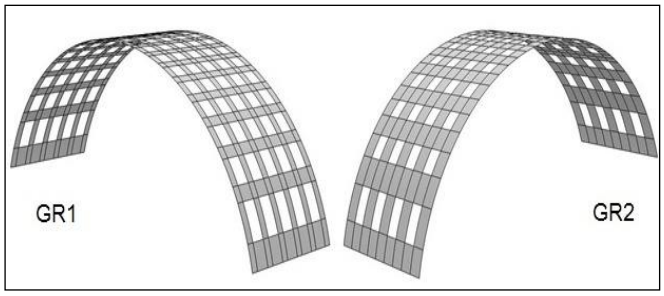

Figure 14: GFRP grids applied to the intrados

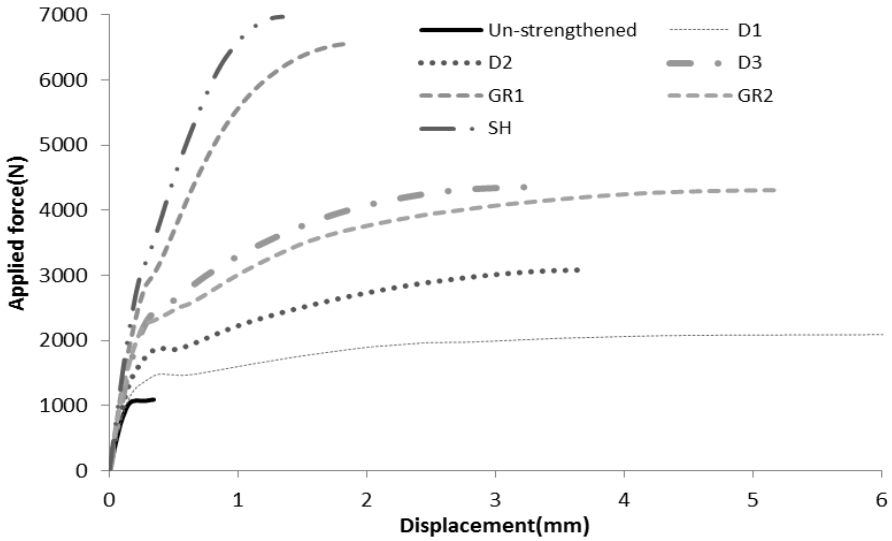

Figure 15: Applied force versus displacement for D, GR and SH models

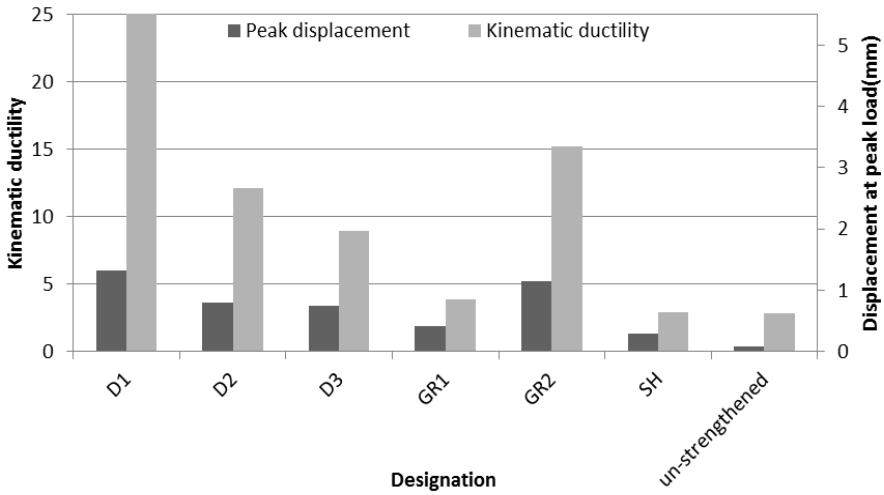

Figure 16: Kinematic ductility/peak displacement versus width of FRP for D, GR and SH models

TABLES

Table 1: Summary of strengthening investigations

Study	Type	Description	Outcome
Creazza, et al., 2001	Experimental	Applying steel reinforced composites at the extrados	Increase in peak load 1200% to 3200%
		Applying steel reinforced composites at the intrados	Increase in peak load 2200% to 3000%
Bati and Rovero, 2008	Experimental	Applying FRP with different widths to the intrados	Increase in peak load 690% to 1362%
		Applying FRP with different widths to the extrados	Increase in peak load 1200% to 1808%
Cancelliere, et al., 2010	Experimental	Strengthening damaged masonry arches with FRP	Increase in peak load 800% to 1300%
	Numerical		Increase in peak load 800% to 1000%
Borri, et al., 2011	Experimental	Applying FRP to the intrados with and without anchorage	Increase in peak load 485% to 1150%

Table 2: Material properties of masonry and GFRP used in numerical modelling (Basilio, 2007)

Element	E(N/mm^2)	υ	Tensile strength(N/mm^2)	Compressive strength(N/mm^2)	Fracture energy G_f (N/mm^2)
Masonry	5000	0.2	0.18	7.8	0.03
GFRP	80000	0.2	1470	-	-

Table 3: Details of reinforcement in numerical models for locally strengthened arches

Designation	Reinforcement direction	No. of strips	Width of strips (mm)	Length of strips (mm)
LL1	longitudinal*	1	50	910
LL2	longitudinal	1	100	910
LL3	longitudinal	1	200	910
LL4	longitudinal	2	25	910
LL5	longitudinal	2	50	910
LL6	longitudinal	2	100	910
LT1	transverse	1	50	450
LT2	transverse	1	100	450
LT3	transverse	1	200	450
LT4	transverse	2	25	450
LT5	transverse	2	50	450
LT6	transverse	2	100	450

*Direction of span is defined as longitudinal direction.

Table 4: Details of reinforcement in numerical models for intrados-strengthened arches

Designation	No. of strips	Width of strips (mm)	Length of strips (mm)
IN1-1	1	50	2015.85
IN1-2	1	100	2015.85
IN1-3	1	200	2015.85
IN2-1	2	25	2015.85
IN2-2	2	50	2015.85
IN2-3	2	100	2015.85

Table 5: Details of reinforcement in numerical models for extrados-strengthened arches

Designation	No. of strips	Width of strips (mm)	Length of strips (mm)
EX1-1	1	50	2083.05
EX1-2	1	100	2083.05
EX1-3	1	200	2083.05
EX2-1	2	25	2083.05
EX2-2	2	50	2083.05
EX2-3	2	100	2083.05

Table 6: Details of reinforcement in numerical models of intrados-strengthened arches with various arrangements

Designation	No. of strips		Length of strips (mm)	Width of strips (mm)
D1	2		2015.85	25
D2	2		2015.85	50
D3	2		2015.85	100
SH	1		2015.85	450
GR1	Longitudinal	6	2015.85	25
	Transverse	20	450	25
GR2	Longitudinal	5	2015.85	50
	Transverse	15	450	50

Table 7: Numerical results in brief for the most efficient IN, D and GR models

Designation	Increase in peak load (%)	Increase in peak displacement(%)	Increase in kinematic ductility(%)	U.F. ($N/mm^4 \times 10^{-4}$)	Price (£/m)	Overall point
IN2-2	214.55	864.71	251.24	2.84	149.85	**1464.65**
D2	182.54	967.65	327.92	5.80	321.68	**1736.43**
GR2	295.05	1420.59	437.46	1.50	907.17	**1395.93**